PREFERENTIAL FLOW DETERMINATION IN A SOIL WITH PETROCALCIC HORIZON BY ELECTRICAL RESISTIVITY TOMOGRAPHY

P. Weinzettel[1,2] , S. Dietrich[1,3], M. Varni[1]

[1] Universidad Nacional del Centro de la provincia de Buenos Aires (UNCPBA).
[2] Comisión de Investigaciones Científicas de la provincia de Buenos Aires (CIC).
[3]Becario del CONICET.
Instituto de Hidrología de Llanuras, Rep. de Italia 780, 7300 – Azul, Bs. As., Argentina. Email: paw@faa.unicen.edu.ar

ABSTRACT. It has been demonstrated that Electrical Resistivity Tomography (ERT) is a suitable tool to obtain 2D views of subsurficial study objects. Its application during an infiltration trial allowed observation of resistivity changes all along a transect. Subsequently, by means of laboratory experiments, resistivity values were converted to soil water content, yielding an evolution of infiltration and drainage. Infiltration test was carried out on a paleudol soil with a 90 cm depth petrocalcic horizon, that shows lateral and vertical discontinuities. Such soils are very common among different zones of Buenos Aires province in Argentina, and impose, in certain cases, some restriction to water flow and development of plant roots. Therefore, knowledge of petrocalcic horizon arrangement, its discontinuities and its hydraulic properties are the objectives of this work. This indirect methodology, which does not disturb the object of study, yields very acceptable results. Resistivity data, later converted in water content values by means of laboratory experiments, have been validated with field measurements of wetness and tensiometry. Tomographies showed clearly a more importante flow of water in those zones where petrocalcic discontinuities are more evident. Based on calculated water content and field matric potencial, some values of hydraulic conductivity and flux were obtained, for different zones of the transect.

RESUMEN. La tomografía de resistividad eléctrica ha demostrado ser una herramienta cuya aplicación permite obtener una visión bidimensional del objeto de estudio con muy buenos resultados. Al aplicarla durante un ensayo de infiltración fue posible observar las variaciones de resistividad de la sección a lo largo del tiempo. Posteriormente, mediante experiencias realizadas en laboratorio las resistividades han sido convertidas en valores de humedad y de esta manera se ha seguido la evolución de la infiltración y el drenaje. El ensayo se realizó sobre un suelo paleudol con presencia de niveles petrocálcicos discontinuos tanto lateralmente como en profundidad presentes a partir de los 90 cm. Este tipo de suelo es muy común en diferentes zonas de la pampa húmeda argentina, produciendo en algunos casos una limitante para la infiltración del agua y el desarrollo de las raíces de los cultivos. Conocer su disposición en profundidad, determinar las discontinuidades que presenta y sus propiedades hidráulicas son los objetivos de este trabajo. Esta metodología indirecta, que no disturba el suelo bajo estudio, ha producido resultados sumamente aceptables. Las medidas de resistividad convertidas en valores de humedad, a partir de las funciones obtenidas en laboratorio, han sido validadas con mediciones *in situ* de humedad y tensión. Las tomografías muestran con suma claridad un flujo mayor de agua por aquellas zonas donde se encuentran las discontinuidades más importantes de los niveles petrocálcicos. A partir de los datos de humedad obtenidos en la tomografías y la tensión matricial del suelo se obtuvieron valores para la conductividad hidráulica y el flujo para distintas zonas del perfil longitudinal de 11 m de extensión.

1.- Introduction

Significant progress has been made in electrical resistivity methods to characterize soils, the unsaturated zone and aquifers. They allow examination of lateral and vertical migration of solutes and pollutants as well (Wendroth et al., 2006).

Development of new high-sensitivity multielectrodic equipments allows measurements of subsurface resistivities without disturbing the medium (Samouëlian et al., 2005; Batlle-Aguilar et al., 2009). Upon surveying a continuous 2D resistivity section, soil heterogeneities are exposed, being petrocalcic horizons a good example of it (Schwartz et al., 2008¸ Weinzettel et al. 2009).

Electrical resistivity is an intrinsic property that depends on composition and arrangement of soil particles, water and salts content and temperature (Rhoades et al., 1989). Therefore, it is of great importance, starting from laboratory tests, to obtain functions, for each soil under investigation, relating resistivity and water content, regarding pore solution conductivity.

Taking these facts into account, the purpose of this work is to generate resistivity – water content soil horizon in order to apply them to measurements taken with a resistivimeter during an infiltration test. Then, another objective was to quantify flow velocities in different points of the transcect and determine zones with preferential flow.

2.- Methodology

2.1.- Site of study

Infiltration tests were carried out on a soil with petrocalcic horizon at 90 cm depth, located in Azul city, Buenos Aires province, Argentina (36º 46' S; 59º 53' W).

This soil has been classified as petrocalcic Paleudol (Soil Survey Stuff, 1999). At the top part of the soil profile a loamy A horizon with moderate to strong structure extends up to 18 cm depth. Below it lays AB horizon, from 18 to 30 cm depth, with blocky structure, underlaid by Bt horizon, of prismatic structure that extends from 30 to 46 cm. BC horizon extends from 46 to 80 cm exhibite prismatic structure parting to blocky. Finally, from 80 to 146 cm, it could be observed a C horizon, masive and friable.

Soil profile exhibits a petrocalcic horizon between 100 and 130 cm depth. It has variable thickness and lateral discontinuities due to different degrees of calcium carbonate cementation. Table 1 shows textural characteristcs of the described soil.

Table 1. Soil texture and bulk density.

Depth (cm)	Clay (%)	Silt (%)	Sand (%)	Bulk density ($g.cm^{-3}$)
20	32.0	34.2	33.8	1.276
30	54.0	28.9	17.2	1.358
60	13.9	56.2	29.9	1.318
90	8.5	56.0	35.5	1.349
120	8.2	45.0	46.8	1.401
150	8.8	43.4	52.2	1.420

2.2.- Infiltration tests

A 11.2 m long transect was selected to carry out an infiltration test. Resistivity measurements were conducted during irrigation by means of 56 electrodes AGI SuperSting R1/IP resistivimeter (AGI, 2005a). Electrodes were placed 20 cm-apart along the transect allowing a depth of investigation of about 2.5 m below the surface. Former tests (Dietrich et al., 2009) showed dipole-dipole as the best array to define vertical structures. Field apparent resistivities were inverted using EarthImager 2D (AGI, 2005b), which converts those resistivities into real ones. At this opportunity, Time Lapse module was employed, which starts each tomography inversion with the same *a-priori* model. Furthermore, a true resistivity section is allowed as the starting model. In this way, inversion artifacts are eliminated and changes in resistivity are referred to the first tomography.

The selected transect was implemented with 15, 30, 60, 90 and 150 cm depth tensiometers at two positions, 3.3 and 8.3 m off the beginning (position 1 and 2 from here on). In addition, at position 2, four TDR probes were placed at four different depths intervals, namely: 0-15, 30-45, 55-70 and 75-90 cm (Fig 1). After that, volumetric water content could be measured at each interval. Surface temperature was also measured and was used for correcting resistivity values (Orellana, 1982).

Upon ending field instrumentation, and before irrigation beginning, an ERT was measured in order to know initial soil condition. After that, irrigation started at a pumping rate of about 3.6 $m^3.h^{-1}$ until a 1000 mm depth was achieved. Pumping was not continuous during the eight days of irrigation and had to be stopped once soil infiltration capacity was exceeded. In total, nineteen tomographies were conducted, one without irrigation, twelve during it and six once irrigation ended, so that drainage could be evaluated

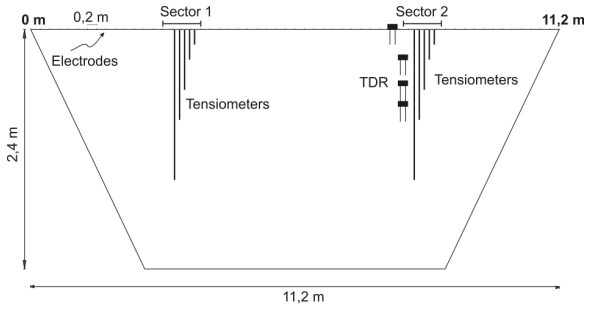

Fig. 1. Diagram showing implemented tensiometers and TDR probes.

2.3.- Laboratory experiments.

Undisturbed soil samples were tried out in order to obtain resistivity-soil water content functions. Samples were collected few meters away from irrigated zone by digging four different horizons of the entire soil profile. Three samples come from the upper A, B and C horizons and an additional one that represents the interval between 120 and 180 cm depth. Before resistivity was measured, samples were washed out with KCl-solutions with five different electrical conductivities, until inward and outward water had the same conductivity. Tried soil water conductivities were as follow: 0.6, 1.0, 1.5, 2.5 and 3.5 $dS.m^{-1}$. Once the whole pore volume was filled with the desired solution conductivity, resistivity measurements were taken while varying water content by drying the samples. Soil moisture was controlled with a 1/100 g precision balance. Resistivity measurements were done using a Wenner array and by rotating the electrodes, eight values of resistivity were obtained for each value of humidity (Gupta and Hanks, 1972). Resulting curves from these laboratory trials allowed to turn resistivity into soil wetness values, for each one of soil horizons.

Laboratory results were fitted following Archie's generalized law, after Shah and Singh (2005). According to these authors, bulk soil electrical conductivity, σ_b, relates with soil solution conductivity, σ_w, and volumetric wetness, θ, as follows:

$$C_b = c \cdot C_w \cdot \theta^m \qquad (1)$$

where c and m are fitting parameters in the sense of Archie's original law (Archie, 1942). If σ_b/σ_w ratio is plotted against water content a power function is obtained where both constants can be obtained easily. Many researchers have investigated the effects of surface conductivity on different lithologies (Rhoades et al., 1989).

Many researchers have investigated the effects of surface conductivity on different lithologies (Rhoades et al., 1989). Since this new law dispenses with this effect upon bulk

conductivity, they hold the opinion that σ_s, will be included in both *c* and *m* parameters.

EarthImager 2D allows obtainment of resistivity logs in whichever point of the section. Such logs were extracted for the TDR probes coordinate. By introducing these data, along with Archie's fitting parameters, in Eq. 1, a σ_w profile could be obtained for each time a tomography was carried out. These σ_w values were then applied for water content assessment in the whole section. It is worth remarking that σ_w affects greatly the bulk soil conductivity value and can not be disregarded.

2.4.- Calculation of $K(\theta)$

Once resistivity sections were turn into soil water content, hydraulic conductivity $K(\theta)$ could be calculated starting from tomographies performed during drainage stage (not shown here). Evapotranspiration was disregarded because low temperatures prevailed in this time of year. Calculations were based on Hillel et al. (1972) method, applying some simplification proposed by Villagra et al. (1994). Results are expressed in the form of Eq. 2.

$$K(\theta) = a \cdot exp(\theta b) \qquad (2)$$

3.- Results

Conducted tomographies manifested changes in resistivity with time as infiltration progressed. Figure 2 shows five selected sections to depict the results.

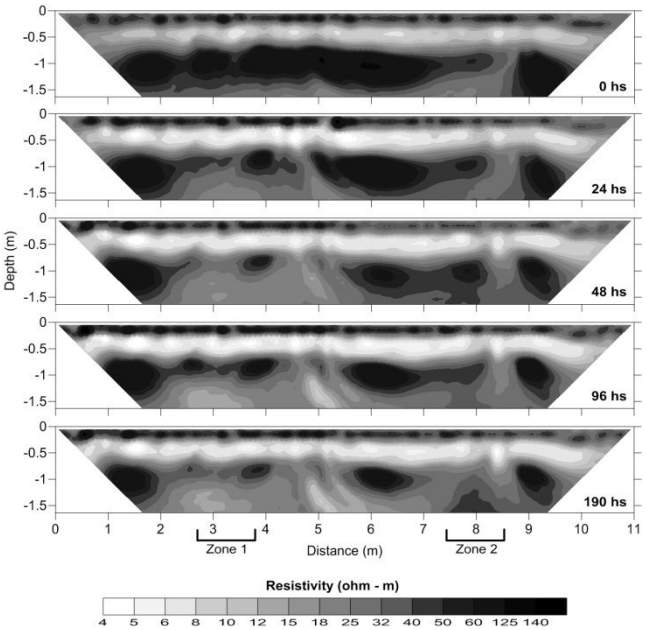

Fig. 2. Selected tomographies conducted during infiltration stage. Values of resistivity are in ohm-m.

As it was expected, in the first resistivity section were found the greatest resistivities because irrigation had not yet started and soil horizons can be clearly observed. Top layer, up to 20 cm depth, shows high resistivities owing to its low water content and high grass roots proportion. By contrast, underlying B horizon has lower resistivities because of its high clay content in its composition which allows it to retain large amount of water. Below it, lies C horizon, with a silty loam texture containing calcium carbonate concretions. The entire soil profile overlies a petrocalcic horizon composed mainly of silty sediments cemented with calcium carbonate, which has certain regional continuity.

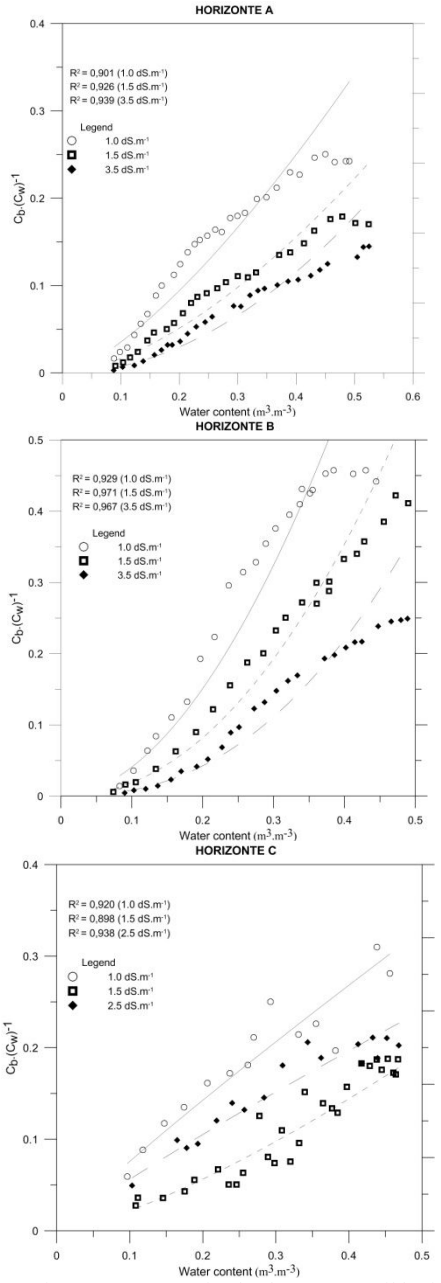

Fig. 3. σ_b/σ_w against water content for the three upper soil horizons.

Despite of that continuity, this extremely firm and compact layer is heterogeneous in its internal constitution since the cementation degree varies within short distances. Regions with lesser amount of calcium carbonate have lower resistivity values and are clearly exposed in sections of Fig. 2. This carbonate layer extends downwards alternating with sandy silts up to the aquifer and decreasing

its carbonate content.

Since resistivity is a property that is also influenced both by lithology and salinity of soil solution, a proper relationship for each horizon is needed which can turn true resistivities into water content values. Such functions were obtained by means of laboratory experiments as was already mentioned, and are exhibited in Figure 3.

For sake of simplicity, only three curves are shown in each chart with their corresponding R-squared coefficient. In addition, curves belonging to 120 – 180 cm depth were left aside because of their resemblance with C horizon. Parameters *c* and *m,* resulting from the mean value of the whole set of curves, are listed in Table 2.

Table 2. Values for *c* and *m* parameters after laboratory experiments.

Horizon	c	m
A	0.858	1.573
B	3.138	2.312
C	0.522	1.056
120 – 180 cm	0.571	1.123

Upon applying laboratory functions, water content sections were calculated taken into account lithology and salinity of pore solution. Figure 4 illustrates these results.

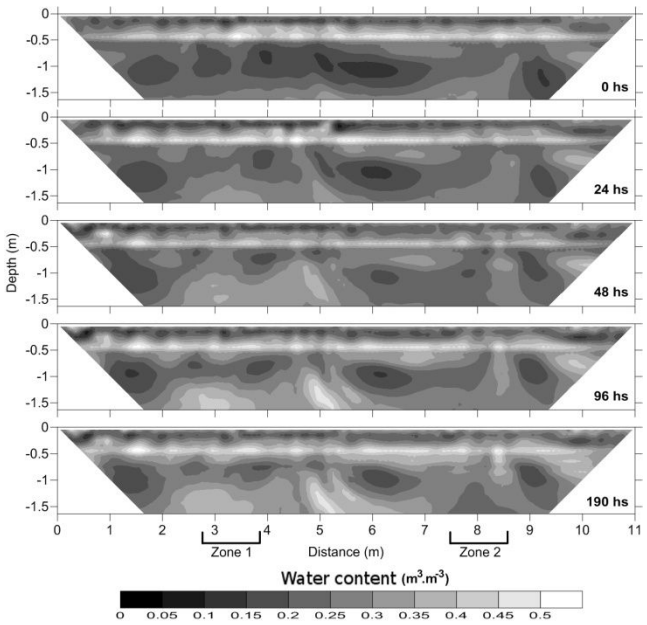

Fig. 4. Sections of soil water content indicating soil moisture during infiltration stage.

A general wetting of the unsaturated zone can be seen clearly, but this wetting is not homogeneous at all. There are some regions of preferential water flow that become more evident at petrocalcic layer depth. The most important ones are those located at 5.0 and 8.5 m from the beginning of the *x* coordinate. Nevertheless, there is a rapid wetting below one meter depth at *x = 3* m, and no preferential path is observed crossing through petrocalcic layer. A tensiometer, located just right there, confirmed this fact indicating that saturation was accomplished before the upper 90 cm – level did. In that way, a matric water flow can be distinguished from a preferential and rapid one and which, in turn, allows to explain water table rises that succeeded without a whole saturation of soil pore space (Weinzettel y Usunoff, 1999).

3.1.- *K(θ)* assessment based on drainage stage

By using those tomographies performed during drainage stage as already mentioned above, *K(θ)* evaluation was done based on the Hillel et al. (1972) method. Three *K(θ)* profiles are shown in Fig. 5.

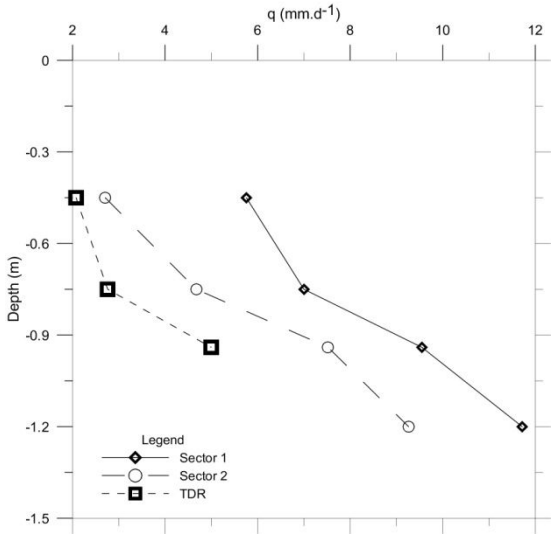

Fig. 5. *K(θ)* profiles for two different sectors in the transect.

Upon extracting resistivity logs, one for sector 1 and another for sector 2, hydraulic conductivity profiles can be obtained and comparisons made. A *K(θ)* profile was also obtained after TDR-measured water content as a means of validation of former profiles. Values are listed in Table 3.

It is worth reminding that TDR measurements were taken in sector 2 and therefore some similarities should be observed. In fact, there is certain concordance between these two profiles suggesting a good assessment of soil water content all along the profile.

Some differences arose after comparison of both calculated profiles, indicating greater hydraulic conductivity in sector 1.

4.- Discussion

4.1.- Laboratory experiments

It has been proved the importance of having good laboratory function in order to obtain reliable water content values, starting from resistivities. As it was previously mentioned, soil solution conductivity, σ_w, cannot be disregarded when it comes to carrying out such experiments because its great contribution to bulk soil conductivity. The magnitude of such contribution should be clear after analyzing charts in Fig. 3.

Table 3. Eq. 2 parameters; saturated field hydraulic conductivity, *Ko* (mm.d^{-1}); maximum field wetness, θo (m^3.m^{-3}); and flux, *q* (mm.d^{-1})

Depth	*a*	*b*	*Ko*	θo	*q*
Sector 1					
-0.45	3.63E-07	40.95	15.92	0.43	5.76
-0.75	1.21E-05	51.62	9.15	0.26	7.00
-0.94	2.48E-04	38.96	16.49	0.28	9.55
-1.2	3.72E-09	57.36	20.24	0.39	11.72
Sector 2					
-0.45	4.39E-15	79.30	3.68	0.43	2.71
-0.75	2.53E-04	23.02	3.06	0.41	4.68
-0.94	7.80E-05	39.25	12.99	0.31	7.52
-1.2	5.41E-12	102.89	16.00	0.28	9.26
TDR					
-0.45	2.47E-17	83.35	1.41	0.46	2.07
-0.75	3.00E-17	104.80	1.80	0.37	2.76
-0.94	2.88E-10	50.27	8.63	0.48	5.00

As explained before, in opportunity of methodology section, *c* and *m* parameters, as long with TDR-measured moisture and conductivities coming from tomographies, were used to get a σ_w profile. Then, this profile was extrapolated to the rest of the tomography and, by means of Arhie's law, entire water content section was calculated. In a former work (Weinzettel et al., 2010), resistivity – water content functions were applied directly by supposing a probable σ_w value for each horizon. This new approach incorporates TDR - measured moisture as a means of correcting soil water content calculations and takes into account soil water conductivity. It is a way of having a notion of σ_w values when this type of data lacks. Collecting a soil water directly with a suction sampler is, undoubtedly, a better way and should be considered when it comes to planning such field experiments.

Another interesting remark about laboratory tests has to do with Archie's parameters. Because of the empirical nature of this law, the fitting constants must be obtained experimentally. These laboratory tests have provided *c* and *m* values for each horizon as a means to characterize each lithology (Table 2).

Archie's *c* constant relates to the conductivity of the solid phase and should be greater when high clay proportion exists. On the other hand, *m* parameter is linked with tortuosity of the pore space and therefore, has an important effect on water flow (Shah and Singh, 2005). These theoretical facts agree with experimental results. Major values of these parameters correspond with B horizon, due to its great clay proportion. Besides having greater surface conductivity, arrangement of clay particles tends to be more disordered, increasing the *m* value. Following this reasoning, C horizon has the lowest constant values. On one hand, it has lesser amount of clay particles and, on the other hand, is sandy silt textured which, in turn, results in less tortuous pore spaces. Horizon A has a middle position between the two cases analyzed.

4.2.- Preferential path of flow

Calculated hydraulic conductivities indicate a general low matric flow, especially at B horizon. Its high clay content makes water flow extremely difficult and even more, due to the expansive nature of these soil components.

Below 65 cm depth, *K(θ)* values increase, being associated with a decreasing in clay content and lithological changes. Edaphic processes are less important at this point, and parental sediment features are better preserved. Even though these sediments are sandy silts, and higher hydraulic conductivities would be expected, calcium carbonate present as cement reduces pore space to a great extent. Nevertheless, reduction in pore volume is, by far, heterogeneous, remaining zones of different *K(θ)*. Moreover, these changes can take place within very short distances.

In short, zones with lesser amounts of calcium carbonate may become a preferential path to infiltration water. And this is precisely what could be observed with ERT surveying. Such zones, upon having a great pore space, can lodge more water, lowering its bulk resistivity. Three preferential water paths are easily shown by tomographies, located at 3, 5 and 8.5 m from the beginning of the section.

Some water flux values were calculated following the Hillel et al. (1972) method, for those zones where tensiometers were available. Water contents coming from TDR were also used to get an additional profile that can be compared with sector 2 values. From both Fig. 5 and Table 3, it is clear that similarities exist between *K(θ)* profiles, obtained after TDR measurements and resistivity conversions. Such resemblance constitutes a way to demonstrate a validation of calculated water content values, because the matric potentials used were the same. Notwithstanding, some differences, especially at 90 cm depth, arise upon observing moisture values, even though both profiles are very close each other. This observation is supported by the heterogeneous nature of petrocalcic horizon, as has just been said.

In spite of lower water content, Sector 1 profile indicates a higher water flux, *q*, in comparison with Sector 2. Obviously, this is related to higher hydraulic conductivities. This was proved by data coming from tensiometers, which indicated a more rapid saturation at sector 1.

4.3.- Inversion process

As explained before, apparent resistivities were turn into real ones by means of Time Lapse inversion module, coming with EarthImager 2D code. It has the advantage of allowing selection of a true resistivity section as the starting model and using it in the successive tomographies. In this way, inversion artifacts are eliminated and a more coherent resistivity evolution can be obtained (AGI, 2005b).

In a former work (Weinzettel et al., 2010), data inversion was done without Time Lapse module and some differences can therefore be observed in the results, because *a-priori* model has a great effect on final true resistivity section. This also affect calculated water content values and, in turn, hydraulic conductivities derived from them.

5.- Conclusions

An infiltration trial was carried out on a petrocalcic paleudol soil with a petrocalcic horizon at 90 cm depth downwards.

Electrical tomography was then applied in order to follow the soil moisture evolution all along a transect selected for the field experiment. Data acquisition was done by using a resistivimeter AGI SuperSting R1/IP, which was able to detect small resistivity changes.

Apparent resistivities collected in the field were inverted with EarthImager 2D code and Time Lapse module, which allows to select an inverted section as an *a-priori* model and to use it in successive tomography inversions. Since the starting model influences to a great extent the final result, inversion artifacts are eliminates by using always the same. In such a way, changes can easily be referred to the first tomography and therefore, it is a very suitable tool to follow the evolution of resistivity in the same place.

Generalized Archie's law was used to convert resistivities into soil water content. Data needed to this law application came from laboratory experiments and TDR – measured moisture. In addition to allowing water content assessment, *c* and *m* fitting parameters were obtained.

Once converted to soil water content, tomographies showed clearly the evolution of moisture with time. Additionally, preferential flow path could be observed very clearly, especially at petrocalcic horizon depth.

6.- References

Advanced Geosciences, Inc., 2005a. *The Super Sting Instruction manual*, 87 p.

Advanced Geosciences, Inc., 2005b. *EarthImager 2D, resistivity and IP inversion software, version 2.2.8. Instruction manual*. Austin Texas.

Archie, G.E., 1942. The electrical resistivity log as an aid in determining some reservoir characteristics. *Transactions of the American Institute of Mining and Metallurgical Engineers, 146:* 54–62.

Batlle-Aguilar, J., Schneider, S., Pessel, M., Tucholka, P., Coquet, Y. and Vachier, P. 2009. Axisymetrical Infiltration in Soil Imaged by Noninvaseve Electrical Resistivimetry. *Soil Sci. Soc. Am. J.* 73:510-520

Dietrich S., P Weinzettel and M. Varni, 2009. Aplicación de tomografía eléctrica para la caracterización de la zona no saturada utilizando distintos espaciamientos electródicos. *VI Congreso Argentino de Hidrogeología, Asocación Internacional de Hidrogeólogos Grupo Argentino, Santa Rosa, La Pampa. Tomo I*, 339-347.

Gupta, S.C. and Hanks, R.J. 1972 Influence of water content an electrical conductivity of the soil. *Soil Sci. Soc. Am. J. 36:855-857.*

Hillel, D., Krentos, V. and Stylianou Y. 1972. Procedure and test of an internal drainage method for measuring soil hydraulic characteristics in situ. *Soil Sci., 114*: 395-400.

Orellana, E. 1982. *Prospección geoeléctrica en corriente contínua.* Paraninfo. Madrid. 578 p.

Rhoades, J.D., Mantegui, N.A., Shouse, P.J. and Alves, W.J. 1989. Soil Electrical Conductivity and Soil Salinity: New Formulations and Calibrations. *Soil Sci. Soc. Am. J. 53*:433-439.

Samouëlian, A., I. Cousin, A. Tabbagh, A. Bruand and G. Richard, 2005. Electrical resistivity survey in soil science: a review. *Soil Till Res 83,* 173-193.

Schwartz, B.F., M.E. Schreiber and T. Yan, 2008. Quantifying field scale soil moisture using electrical resistivity imaging. *J. of Hydrology, 362*, 234-246

Shah, P.H., and Singh, D.N., 2005. Generalized Archie's Law for Estimation of Soil Electrical Conductivity. *J. of ASTM International, 2 (5).*

Soil Survey Staff. 1999. Soil Taxonomy. A Basic System of Soil. Classification for making and Interpreting Soil Surveys. Agric. Handbook No. 436, 2nd. Edition. NRCS-USDA. US Govern. Printing Office Washington, D.C.

Villagra, M., Michiels, P., Hartmann, R., Bacchi, O. and Reichardt, K. 1994. Field determined variation of the unsaturated hydraulic conductivity functions using simplified analysis of internal drainage experiments. *Sci. Agric. Piracicaba, 51*:133-122.

Weinzettel, P. and Usunoff, E. 1999. "Hidrodinámica de la zona no saturada en suelos argiudoles de la cuenca del arroyo del Azul". Hidrología Subterránea. Tineo, A. ed. *Serie de Correlación Geológica Nº 13* : 297 - 305

Weinzettel, P.; E. Usunoff and L. Vives, 2005. Groundwater recharge estimations from studies of the unsaturated zone. Cap. 11, Pp. 133-143 en: E. Bocanegra, M. Hernández y E. Usunoff (eds.). *Groundwater and human development*. Balkema Publishers, Londres, Inglaterra. 300 p.

Weinzettel, P., Dietrich, S. and Varni, M. 2009. Utilización de tomografía eléctrica con distintas configuraciones y espaciamientos electródicos para la caracterización de la zona no saturada. Pp. 253-260. *In*: Silva Rojas, O. y Carrera Ramírez, J. ed. *Jornadas de Investigación de la zona no saturada del suelo, 9*, Barcelona, España.

Weinzettel, P., M. Varni, S. Dietrich and E. Usunoff, 2009. Evaluación de tres dispositivos de tomografía eléctrica para la identificación de horizontes petrocálcicos en el suelo. *Ci. Suelo 27(1)*:135-146

Weinzettel, P., Dietrich, S. and Varni, M. 2010. La infiltración del agua en el suelo y zona no saturada a partir de mediciones de resistividad. I Congreso Internacional de Hidrología de Llanuras. Azul, Buenos Aires. Tomo I, 333-340.

Wendroth, O., Koszinski, S. and E. Pena-Yewtukhiv, E. 2006. Spatial association among soil hydraulic properties, soil texture, and geoelectrical resistivity. *Vadoze Zone J. 5*, 341-355.